3074–3082 *Nucleic Acids Research, 2009, Vol. 37, No. 9* *Published online 20 March 2009*
doi:10.1093/nar/gkp177

A role for hydrophobicity in a Diels–Alder reaction catalyzed by pyridyl-modified RNA

Keith T. Gagnon[1], Show-Yi Ju[2], Michael B. Goshe[1], E. Stuart Maxwell[1] and Stefan Franzen[2,*]

[1]Department of Molecular and Structural Biochemistry and [2]Department of Chemistry, North Carolina State University, Raleigh, NC 27695, USA

Received December 20, 2008; Revised March 1, 2009; Accepted March 2, 2009

ABSTRACT

New classes of RNA enzymes or ribozymes have been obtained by *in vitro* evolution and selection of RNA molecules. Incorporation of modified nucleotides into the RNA sequence has been proposed to enhance function. DA22 is a modified RNA containing 5-(4-pyridylmethyl) carboxamide uridines, which has been selected for its ability to promote a Diels–Alder cycloaddition reaction. Here, we show that DA_TR96, the most active member of the DA22 RNA sequence family, which was selected with pyridyl-modified nucleotides, accelerates a cycloaddition reaction between anthracene and maleimide derivatives with high turnover. These widely used reactants were not used in the original selection for DA22 and yet here they provide the first demonstration of DA_TR96 as a true multiple-turnover catalyst. In addition, the absence of a structural or essential kinetic role for Cu^{2+}, as initially postulated, and non-sequence-specific hydrophobic interactions with the anthracene substrate have led to a reevaluation of the pyridine modification's role. These findings broaden the catalytic repertoire of the DA22 family of pyridyl-modified RNAs and suggest a key role for the hydrophobic effect in the catalytic mechanism.

INTRODUCTION

The era of functional nucleic acid discovery began with the realization that RNA could catalyze chemical reactions and bind small molecules with high specificity and affinity (1,2). RNAs with high affinity for other molecules can be generated using an *in vitro* selection technique known as SELEX (3–5). More recently, nucleic acids have been selected for activity in promoting organic reactions in aqueous solution (6,7). Inspiration for artificial ribozymes is derived from the growing variety of known natural ribozymes, such as the well-characterized self-splicing introns and the hammerhead RNA, as well as protein-assisted ribozymes like RNase P and the ribosome and spliceosome (8–13). Natural ribozymes are typically metalloenzymes capable of efficient nuclease activity (14). In general, the catalytic efficiency of artificial ribozymes has been low compared with protein enzymes that catalyze analogous reactions (14,15). Accordingly, *in vitro* selections of nucleic acid catalysts have increasingly employed nucleotides with moieties not found in nature to enhance catalytic potential (16–22). The introduction of artificial functionality is a challenge, since the choice of functional group will have a major impact on the functionality that can be sampled in the selection process.

The choice of side-chain modification strongly influences whether metal chelation or acid–base chemistry will prevail in the reaction mechanism. For example, in a selection for RNAse A activity, an imidazole modified nucleotide in a DNA enzyme was employed to mimic the catalytic role of histidine in proteins (20). However, in this case, micromolar Zn^{2+} concentration was required for activity. Considering the mechanism of RNAse A, which uses lysines and imidazoles to cleave the phosphodiester backbone without requirement for a metal ion, it has been suggested that a strategy employing two functional groups, such as primary amines and imidazole, would serve as a better nuclease (19,23). This strategy permits development of DNA catalysts without a requirement for metal ions that could potentially have application *in vivo* (24).

The search for a ribozyme capable of catalyzing a Diels–Alder reaction provides an early example of the application of modified nucleotides in SELEX. The Diels–Alder reaction is a [4 + 2] cycloaddition of a conjugated diene and a dienophile to form a substituted cyclohexene system (25). The Diels–Alder reaction is important in synthesis strategies since it creates two carbon–carbon

*To whom correspondence should be addressed. Tel: +1 919 515 8915; Fax: +1 919 515 8920; Email: stefan_franzen@ncsu.edu
Present address:
Keith T. Gagnon, Department of Pharmacology, University of Texas Southwestern Medical Center, Dallas, TX 75390, USA

bonds and up to four new stereocenters (26). Initial SELEX experiments aimed at isolating a ribozyme with Diels–Alderase (DAase) activity were successful in binding a transition state analog, but no catalytic DAase activity was found for these molecules (27). However, incorporation of uridines containing a pendant 5-(4-pyridylmethyl) carboxamide group (abbreviated pyridyl, Figure 1A) into the RNA during selection yielded a family of RNAs that could promote the Diels–Alder reaction, the most well-studied being DA22 (21). Of the DA22 family of RNAs, the most active sequence tested thus far is a truncated form of DA22, called DA_TR96 (Figure 1A) (28). These pyridyl-modified RNAs were selected through conjugation of the RNA to the Diels–Alder product (Figure 1B), thereby limiting the reaction to a single turnover (21).

In vitro selection of natural RNA has since yielded unmodified DAase ribozymes, which raises the question as to the role played by pyridines in DA22 function. The most active unmodified RNA isolate capable of catalyzing the Diels–Alder reaction is a sequence designated 39M49, shown in Figure 1C (6). The initial selection of 39M49 also utilized covalent attachment of the substrate but an activity assay with substrates free in solution was later adapted to fully characterize its catalytic potential (6,29). The activity assay relies upon the change in absorbance of the diene, 9-anthracenylmethyl hexaethylene glycol (AHEG), whose absorbance decreases proportionally upon reaction with the dienophile, 6-maleimidocaproic acid (MCA) and formation of Diels–Alder product (Figure 1D). The 39M49 RNA structure, folding and substrate interactions have been well characterized by X-ray crystal structures of the RNA both free and bound to a Diels–Alder product, fluorescence resonance energy transfer (FRET) and photoaffinity cross-linking, among other techniques (30–34).

In addition to RNA, other macromolecules such as DNA, antibodies (abzymes) and even small molecules like cyclodextrin, have been demonstrated to accelerate the Diels–Alder reaction in aqueous solution or in solutions with small amounts of organic solvent (7,35–38). The fact that the hydrophobic effect can produce significant rate enhancements in water calls for careful consideration of the role played by hydrophobic modifications in functional nucleic acids. It is therefore significant that a series of reports described a bimolecular Diels–Alder cycloaddition reaction promoted by full-length pyridyl-modified DA22 (154 nt) with an absolute requirement for Cu^{2+} (21,28,39,40). The selection and analysis conditions for DA22 utilized a bimolecular reaction between a biotinylated maleimide dienophile (BMCC) present in solution at 1000-fold molar excess and an insoluble diene, 2,4-hexadiene, conjugated to the RNA (Figure 1B). However, enzymatic constants reported in these studies, such as k_{cat}/K_m, were not informative since none of the pyridyl-modified RNA sequences has been previously demonstrated to function as multiple turnover catalysts (21,28,39,40).

The low solubility of 2,4-hexadiene in water, as well as the need for assay conditions that permit turnover, led us to test alternative substrates in order to investigate the catalytic activity of DA_TR96. Here, we report the unexpected finding that the most active DA22 truncate DA_TR96 can catalyze the Diels–Alder reaction using the substrates AHEG and MCA, although this substrate pair was not the target of the original *in vitro* selection. A nonessential role for Cu^{2+} ions was observed as well as nonsequence-specific interactions between pyridyl-modified RNA and the anthracene substrate. Structural probing of DA_TR96 RNA revealed no differences between modified and unmodified RNA and a lack of structural changes in the presence of Diels–Alder substrates. The mechanism for rate enhancement by DA_TR96 is proposed to be dominated by hydrophobic interactions of pyridyl groups with substrate molecules.

MATERIALS AND METHODS

RNAs were made by *in vitro* transcription from PCR-generated or synthesized DNA templates essentially as described (28,29,41). For production of modified RNA, 5-(4-pyridylmethyl) carboxamide UTP, analyzed by liquid chromatography-tandem mass spectrometry (Supplementary Figure S2), was substituted for unmodified UTP in standard transcription reactions. RNA concentrations were estimated by absorbance at 260 nm using calculated extinction coefficients.

The procedure for an in-solution Diels–Alder activity assay was similar to that previously described (29). Briefly, RNA (7 μM), AHEG (0.1 mM), and MCA (0.5 mM) were brought up in reaction buffer (30 mM Tris, pH 7.4, 300 mM NaCl, 80 mM $MgCl_2$, 10% ethanol). $CuCl_2$ was included at a final concentration of 20 μM where applicable. Diels–Alder product formation was monitored by absorbance at 365 nm at room temperature ($23 \pm 2^{\circ}C$).

RNAs were thermally denatured in an Applied Photophysics π*-180 spectropolarimeter at a fixed wavelength of 268 nm. Reactions contained 1.5 μM RNA in buffer (20 mM cacodylate, pH 7.2, 75 mM NaCl, 75 mM KCl, 1 mM $MgCl_2$, 10% ethanol) and 0.1 mM AHEG when applicable. Reactions were heated in a cylindrical quartz cuvette at a ramp rate of 1°C/min and a sampling rate of 1000 points for 15 s every 1°C.

RNA structural mapping was carried out as previously described (41). Briefly, 5′-radiolabeled RNA ($\geq 1 \times 10^5$ cpms) in buffer (20 mM HEPES, pH 7.0, 100 mM NaCl, 30 mM $MgCl_2$, 0.2 mM EDTA, 10% ethanol, 10 mg/ml tRNA) was mixed with the indicated amounts of $CuCl_2$ or Diels–Alder substrates. Reactions were combined with mung bean nuclease (0.6 U/μl) or lead acetate (1 mM) for 8 min at room temperature. Reactions were precipitated, resolved on Tris–borate–EDTA (TBE)-buffered 12% polyacrylamide sequencing gels and visualized by phosphorimaging.

RESULTS

DA_TR96 catalyzes a Diels–Alder reaction with new substrates

In order to establish a multiple turnover assay for DA_TR96 shown in Figure 1A, we implemented an

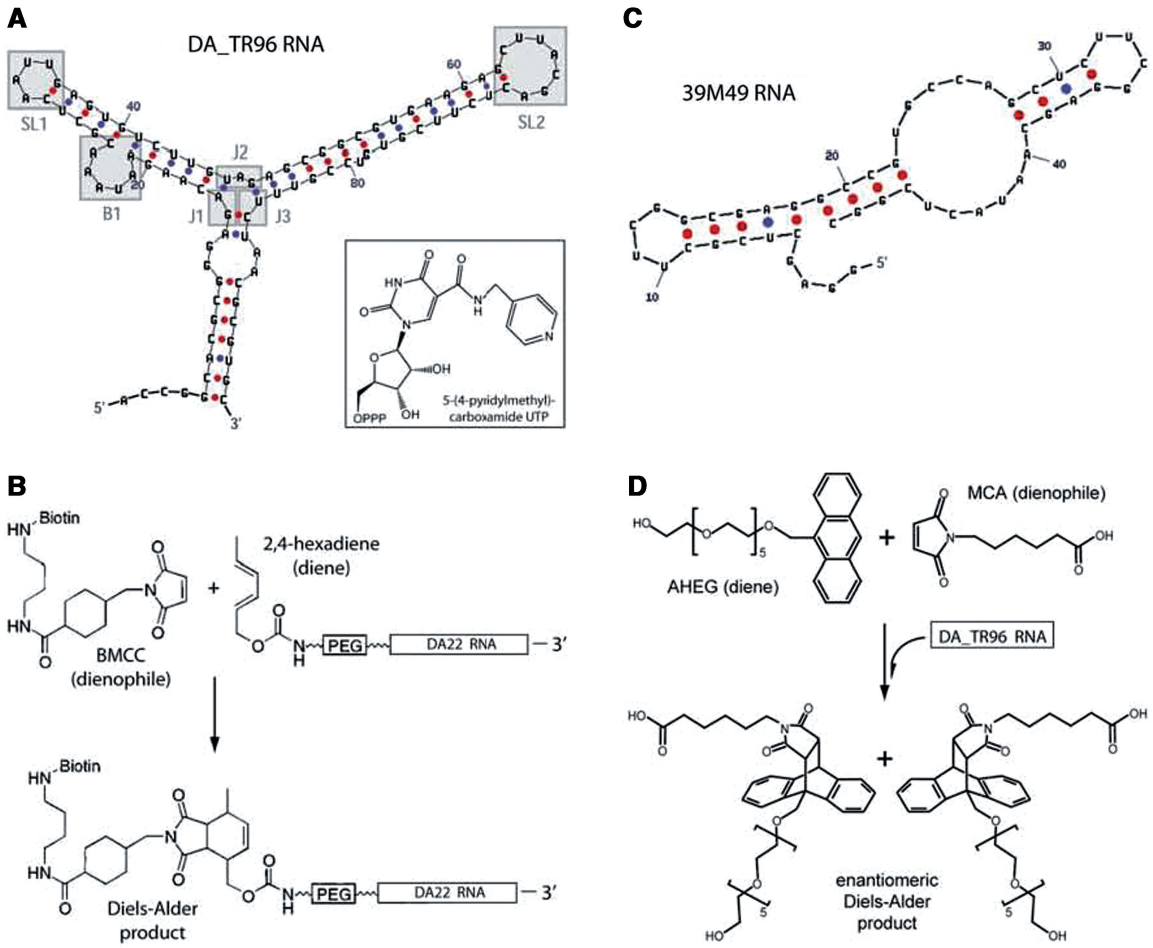

Figure 1. The pyridyl-modified DA_TR96 RNA and the Diels–Alder reactions catalyzed by DA_TR96. (**A**) Primary sequence and predicted secondary structure (44) of the DA_TR96 RNA (28). Inset: chemical structure of pyridyl-modified UTP (pyr-UTP) (21). OPPP; triphosphate moiety; J1, junction 1; B1, bulge 1; SL1, stem–loop 1; J2, junction 2; SL2, stem–loop 2; J3, junction 3. (**B**) Schematic of the DA22 Diels–Alderase selection reaction (21). PEG, polyethylene glycol linker; BMCC, 1-biotinamido-4-[4′-(maleimidomethyl)cyclohexane-carboxamido]butane. (**C**) Primary sequence and predicted secondary structure (44) of the 39M49 RNA (6,29). (**D**) Schematic of the in-solution Diels–Alderase activity assay used here utilizing AHEG and MCA Diels–Alder substrates (29).

absorbance-based assay originally designed for the ribozyme 39M49 shown in Figure 1C (6,29). This assay makes use of an anthracene derivative (AHEG) for the diene and a maleimide derivative (MCA) for the dienophile (Figure 1D). Similar anthracene and maleimide reactants have also been widely used in catalytic assays for the Diels–Alder reaction (6,7,29,37,38). In this activity assay, both diene (AHEG) and dienophile (MCA) are free in solution and Diels–Alder [4 + 2] cycloaddition results in formation of two enantiomeric Diels–Alder products (Figure 1D), which can be monitored by a decrease in anthracene absorbance at 365 nm (A_{365}) as the reaction proceeds.

There is no reason to expect *a priori* that a pyridyl-modified RNA, originally selected *in vitro* with quite different Diels–Alder substrates (Figure 1B), would accelerate a reaction between AHEG and MCA. However, Figure 2A shows that DA_TR96 significantly enhances the Diels–Alder reaction rate. Moreover, Figure 2A also shows that the DA_TR96 control sequence without the pyridyl modification has little catalytic activity. Mass spectrometry analysis confirmed the formation of the expected Diels–Alder product under these reaction conditions (Supplementary Figure S1). The 39M49 RNA also accelerated the reaction between AHEG and MCA as expected, although with an apparently slower rate compared with DA_TR96 (Figure 2A). Notably, Cu^{2+} was not required for DA_TR96 acceleration of the Diels–Alder reaction under multiple turnover conditions. The presence of Cu^{2+} at 20 μM, a concentration previously reported to be essential for the bimolecular reaction of the BMCC dienophile and 2,4-hexadiene conjugated to the RNA (21,39), only moderately enhanced the reaction rate and overall conversion. Likewise, addition of the Cu^{2+}-specific chelator bathocuproine disulfonic acid (BCS) at 100 μM only slightly reduced the reaction rate (Figure S3). The BCS control experiment shows that a trace Cu^{2+} impurity cannot account for activity in reactions where Cu^{2+} was not added. However, a substantially higher Mg^{2+} concentration (80 mM) was required

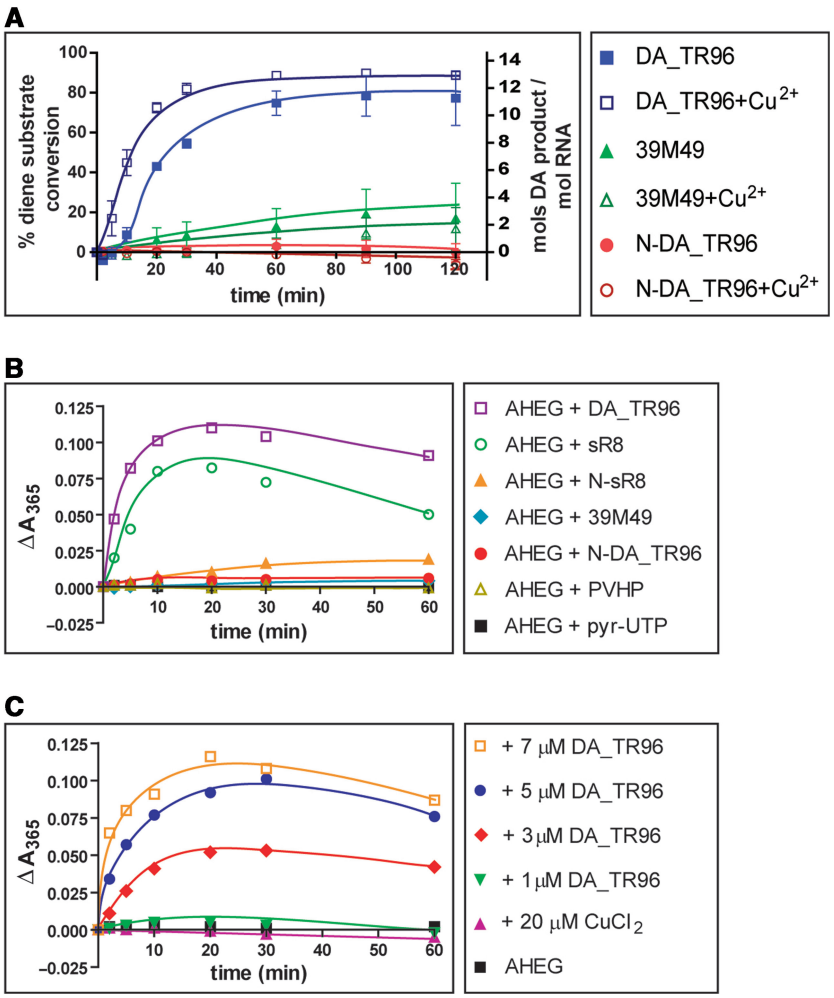

Figure 2. DA_TR96 RNA accelerates the Diels–Alder reaction between AHEG and MCA free in solution and interacts in a nonsequence-specific manner with AHEG. (**A**) Plot of percent substrate conversion (product formation) and enzymatic turnover versus time with and without 20 μM $CuCl_2$. Error bars are standard error of the mean for three replicate measurements. The uncatalyzed reaction values were subtracted as background. (**B**) Plot of the change in absorbance at 365 nm over time for reactions containing 0.1 mM AHEG with various RNAs (at 7 μM) and other components under Diels–Alderase activity assay conditions (no MCA present). N-sR8, native unmodified RNA; sR8, pyridyl-modified RNA. PVHP (1 mg/ml); pyr-UTP, pyridyl-modified UTP (1 mM). (**C**) Plot of the change in absorbance at 365 nm over time for reactions containing 0.1 mM AHEG and increasing concentrations of DA_TR96 RNA up to 7 μM under Diels–Alderase activity assay conditions (no MCA present). Curves shown in the figure are a guide to the eye. Curve fitting to a pseudo-first-order rate constant was performed using nonlinear least squares fit with an exponential association equation in the program Prism (GraphPad).

in our activity assay than was used in the selection (1 mM Mg^{2+}). This observation indicates that, although the reaction does not strictly require Cu^{2+}, it does require divalent metal ions to help coordinate RNA structure and possibly also to stabilize substrate interactions with the RNA.

Interaction of pyridyl-modified RNA with AHEG

It has been shown that the AHEG diene interacts with a well-defined binding pocket of the 39M49 RNA (31). However, the lack of activity for native, unmodified DA_TR96 RNA (N-DA_TR96), having the same sequence as DA_TR96 but synthesized with unmodified UTP, suggested that AHEG may interact with pyridine side chains rather than the RNA itself (Figure 2A). Indeed, we found that the anthracene derivative AHEG interacted with pyridyl-modified RNA in an apparently nonsequence-specific manner. Addition of DA_TR96 to AHEG in standard activity assay conditions (0.1 mM AHEG) but in the absence of the MCA dienophile showed a sharp increase in A_{365} (Figure 2B). This contrasts the reduction in A_{365} that is observed when AHEG, MCA and DA_TR96 are all present and Diels–Alder product is formed (Figure 2A). The increase in A_{365} was not observed when N-DA_TR96 or 39M49 RNAs were incubated with AHEG (42,43). However, an unrelated 68-nt long RNA, called sR8 (41,45), generated the same effect when its uridines were substituted with 5-(4-pyridylmethyl) carboxamide uridines, although it was not active as a catalyst for the Diels–Alder reaction. Conversely, neither 5-(4-pyridylmethyl) carboxamide UTP by itself, nor a short water-soluble pyridine-containing polymer, hydrogenated polyvinyl pyridine (PVHP), reproduced the increase in A_{365}. Therefore, the pyridyl

modification incorporated into RNA is sufficient to cause interaction with AHEG substrate in a nonspecific manner. This interaction appears to rely on the hydrophobic interactions of the anthracene substrate, AHEG, with the pyridyl groups within the RNA scaffold.

The interaction between AHEG and pyridyl-modified RNA was briefly observed during standard activity assays with DA_TR96, where a short increase in A_{365} occurs before a strong decrease in absorbance corresponding to Diels–Alder product formation (Figure 2B and Supplementary Figure S3). Fast conversion of AHEG to Diels–Alder product may compete with this interaction, in agreement with the fact that the interaction between modified RNA and AHEG was found to be concentration dependent (Figure 2C). Although adding pyridyl-modified RNA to AHEG resulted in an increase in A_{365}, the absorbance returned to initial values after several hours of incubation (Supplementary Figure S4A). However, this incubation period resulted in inactivation of either the RNA or the reactant since addition of MCA to the reaction afterwards did not yield an increase in A_{365} (Supplementary Figure S4B). The increase in A_{365} of the AHEG diene may be due to hyperchromism of the anthracene ring upon stacking. The stacking interaction weakens over time, but the structural effect is such that the pyridyl-modified RNA or anthracene substrate is rendered inactive. The observation that the substrate AHEG interacts with DA_TR96 at multiple sites through a nonspecific hydrophobic interaction, which ultimately leads to inactivation of the ribozyme, prevents the application of quantitative enzyme kinetic analysis using the Michaelis–Menten formalism.

Probing the effect of pyridyl modification and Diels–Alder substrates on DA_TR96 structure

Nucleotide base modifications are usually incorporated into RNA and DNA during *in vitro* selection to enhance functionality (5,16–23). Such modifications, especially bulky chemical groups, can potentially alter RNA folding, structure and stability. Although modifications located away from the nucleotide base-pairing face should not substantially interfere with base pairing, they may alter helix stability or formation of higher order or noncanonical structures like triple helices, base-stacking or backbone interactions (16,17,22). To better understand the role of the pyridine modification in RNA structure and function, we analyzed DA_TR96 using RNA structural probing. Unmodified and modified DA_TR96 were radiolabeled and subjected to limited digestion with mung bean nuclease or Pb^{2+}, which both preferentially cleave single-stranded and dynamic RNA, and resolved on polyacrylamide gels. It should be noted that heavy metal ions often generate cleavage patterns that vary from that of nucleases due to differences in probe size and specificity, an important reason for using both probing methods (30,41).

RNA structural mapping with mung bean nuclease was consistent with secondary structure predictions. Features predicted by Mfold using the Zuker algorithm (28,44), shown in Figure 1A, could all be identified. Furthermore, consensus structure predictions using RNAalifold (46) and covariation data from 50 aligned members of the DA22 sequence family (28) yielded an RNA secondary structure very similar to that predicted by Mfold (Supplementary Figure S5). Stem structures, as well as the nucleotides surrounding the putative triple-helix junction, were well protected from cleavage, indicating proper helix formation and stable interactions or folded RNA structure in the junction region (Figure 3A).

While no significant differences in overall structure were found between modified DA_TR96 and unmodified N-DA_TR96, noticeable differences in accessibility of certain elements between the two were observed (Figure 3A and B). Stem-loop 1 of N-DA_TR96 is quite accessible to cleavage, while it is protected in modified DA_TR96. In contrast, stem–loop 2 is more accessible to cleavage in DA_TR96 than in N-DA_TR96. These results might suggest possible long-range interactions between stem–loops 1 and 2, perhaps dependent on the pyridine modification. This is an attractive hypothesis since both loops contain two adjacent pyridyl-modified uridines (Figure 1A). RNA folded structure positioning the pyridine rings in close proximity might allow them to stack. Three helix junctions in RNA have been demonstrated to induce inter-helical interactions between stems, placing stem–loops in close proximity for interaction (47). While the contribution of putative long-range interactions to RNA structure and function is not known, these RNA mapping data are consistent with the hypothesis that pyridyl-modified uridines do not significantly impact the formation of RNA secondary structure. The pyridine modification did, however, reduce thermal stability of DA_TR96, indicating a significant decrease in RNA helix stability (Figure 3C). Thermal denaturation analysis revealed that the melting temperature (T_m) of DA_TR96 was lowered by $\sim$10°C compared with N-DA_TR96 RNA.

RNA structural mapping revealed that Diels–Alder reactants and Cu^{2+} had no significant effect on DA_TR96 secondary structure (Figure 4). Each reactant alone or in combination, as well as in the presence of Cu^{2+}, at standard activity assay concentrations failed to elicit significant changes in the RNA cleavage pattern when probed with both mung bean nuclease and Pb^{2+} (Figure 4). Consistent with our observations, a separate study of the unmodified 39M49 DAase found no significant changes in RNA structure when digested with Pb^{2+} or dimethylsulfate (DMS) in the presence of similar substrates and Diels–Alder product (30). A lack of RNA structural changes in the presence of Diels–Alder reactants does not rule out a specific substrate binding pocket for DA_TR96 but is consistent with a largely nonstructural role for the 4-pyridylmethyl carboxamide base modification in Diels–Alder rate acceleration.

DISCUSSION

Modified nucleotides offer a variety of chemical functionalities that can be incorporated into RNA during *in vitro* selection. For the DA22 family of pyridyl-modified

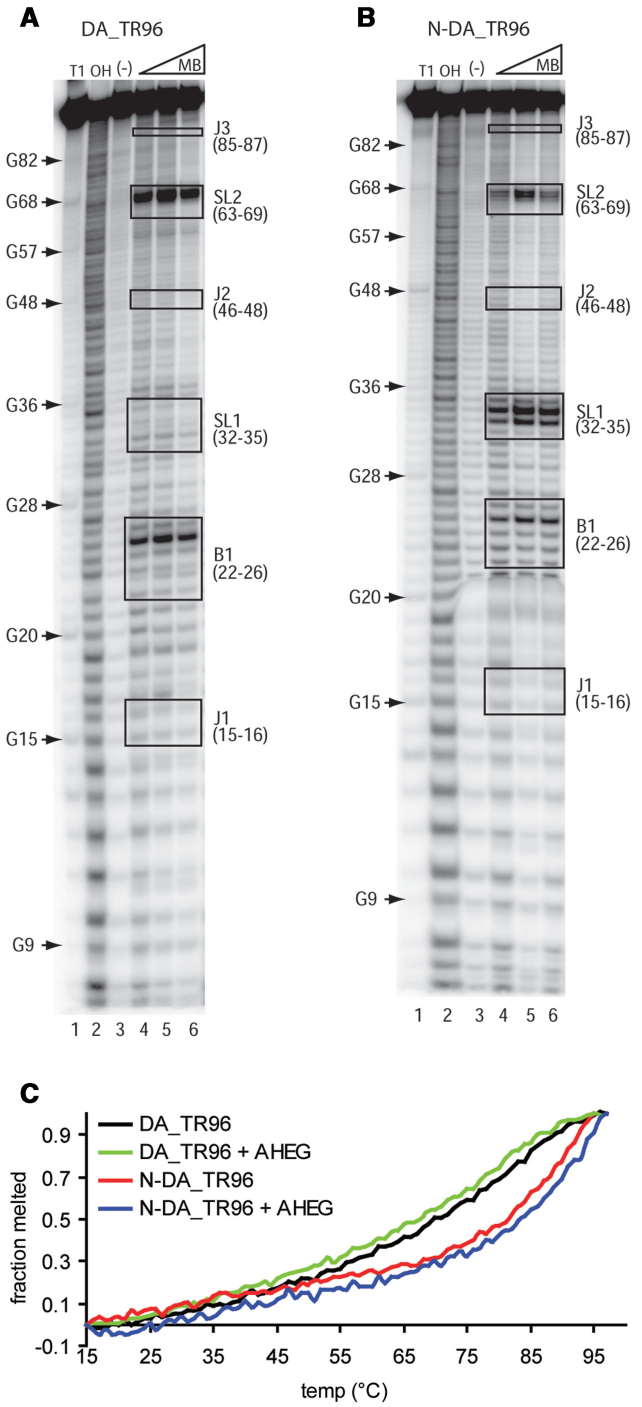

Figure 3. The secondary structures of pyridyl-modified and unmodified DA_TR96 RNAs are similar but the pyridyl modification reduces RNA stability. The secondary structure of (**A**) DA_TR96 and (**B**) N-DA_TR96 (native, unmodified RNA) was mapped using mung bean (MB) nuclease. Increasing concentrations of MB nuclease were titrated with for each 5′-radiolabeled RNA and reactions resolved on a denaturing polyacrylamide gel. Structural elements corresponding to the predicted secondary structure in Figure 1B are boxed and indicated. A T1 RNase digestion ladder is shown in lane 1 and an alkaline hydrolysis ladder in lane 2 to identify RNA primary sequence. (**C**) Thermal denaturation of modified and unmodified DA_TR96 in the absence or presence of 0.1 mM AHEG.

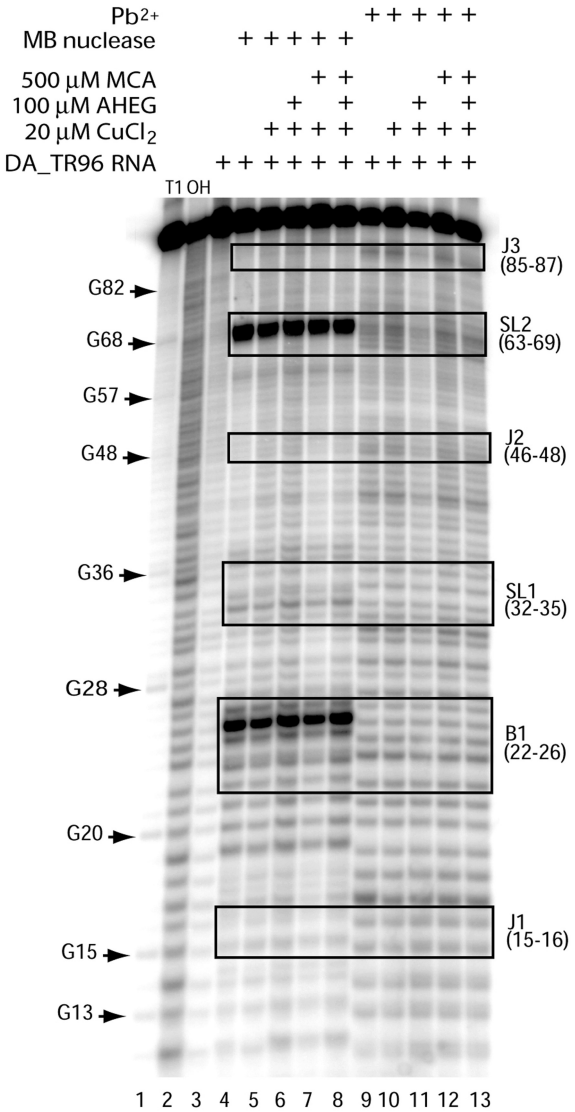

Figure 4. The structure of pyridyl-modified DA_TR96 RNA does not change in the presence of $CuCl_2$ and Diels–Alder substrates. Mung bean (MB) nuclease or lead(II) acetate (Pb^{2+}) was incubated with 5′-radiolabeled RNA and specified reaction components, as indicated above the gel, and reactions resolved on a denaturing polyacrylamide gel. Structural elements corresponding to the predicted secondary structure in Figure 1B are boxed and indicated. A T1 RNase digestion ladder is shown in lane 1 and an alkaline hydrolysis ladder in lane 2 to identify the RNA primary sequence.

RNAs, Diels–Alderase activity has been proposed to arise from Cu^{2+} ion coordination and potentially unique RNA structure or substrate binding due to the presence of the 5-(4-pyridylmethyl) carboxamide modification (21,40). Here, we show that the most active DA22 family member, DA_TR96, functions as a multiple-turnover catalyst using Diels–Alder substrates free in solution that are quite different from those of the original selection. The lack of solubility of the original reactant pair has precluded the observation of multiple turnover catalysis in any of the previous studies (21,28,39,40). Catalytic activity was dependent on the pyridyl modification but did not require Cu^{2+} as an obligatory ion. Nonsequence-specific

interactions were observed between the hydrophobic anthracene derivative AHEG and pyridyl-modified RNA. In terms of the effect of pyridyl-modified uridines on RNA structure, RNA secondary structure was not affected and no significant changes were observed in the presence of Diels–Alder substrates or Cu^{2+} ion. Together, these results raise questions concerning the role of the pyridyl group in the Diels–Alderase activity of the DA22 family of modified RNAs. We propose a role for the pyridyl group in facilitating Diels–Alder catalysis based upon its hydrophobic nature.

Water is known to enhance the Diels–Alder reaction via the hydrophobic effect. For example, the Diels–Alder reaction between an anthracene–maleimide pair similar to that used here has a 200-fold enhancement in water relative to organic solvents (38). The hydrophobic effect provides a driving force for association of the reactants, which is increased on hydrophobic surfaces in water. Cyclodextrin accelerates the Diels–Alder reaction for small molecules that fit into the cavity by a factor of 10 above that in aqueous solution (48). However, the anthracene–maleimide pair is larger than the volume inside a cyclodextrin molecule so that the catalytic rate of the Diels–Alder reaction for this pair is actually decreased in aqueous solution when cyclodextrin is added. On the other hand, the substrate cavity of the 39M49 ribozyme is an excellent fit for the AHEG–MCA substrate pair (31) and the rate enhancement is ~20 000 fold over the rate in water (29). The slower rate of 39M49 compared with DA_TR96 observed here may be due to the well-defined substrate binding pocket, which not only leads to high stereospecificity, but also product inhibition (31,34). Therefore, a nonspecific hydrophobic surface may provide greater catalytic activity than a highly specific binding pocket. It is likely that this type of mechanism explains why DA_TR96 promotes a 5.5-fold acceleration of the Diels–Alder reaction relative to 39M49 for the AHEG–MCA substrate pair based on a fit of each to a single-exponential function as a model for a pseudo-first-order rate constant. The kinetic result can be rationalized by the consideration that the 23 attached pyridyl groups (one for each uridine in the DA_TR96 sequence) can form regions of hydrophobicity stabilized by the three stem–loop scaffold shown in Figure 1A. Although the 3D structure has not been determined, it is reasonable to hypothesize that such a hydrophobic surface of a single DA_TR96 can accommodate multiple AHEG molecules.

The role played by Lewis acidity may be complementary to that played by hydrophobicity. Cu^{2+} acts as a Lewis acid that enhances the rate of the Diels–Alder reaction in water. However, a range a ligands including diamines, phenanthroline and the α-amino acids significantly 'decrease' the catalytic activity of Cu^{2+} in water due to steric hindrance (49). The catalytic rate of the Diels–Alder reaction is nearly the same as for free Cu^{2+}, but the association constant of the substrates with Cu^{2+} decreases by a factor of 10 or even more for bidentate aromatic amines (50). More recent work using a scaffold of double-stranded DNA intercalated by hydrophobic Cu^{2+} chelators has shown, for the first time, an acceleration of the rate of Diels–Alder reactions in solution with significant enantiomeric selectivity (50,51). Hydrophobicity due to solvent exclusion and complex interaction with the major groove of DNA are mitigating factors that can offset the steric hindrance of Cu^{2+} ligation and give a modest rate enhancement. Although Cu^{2+} does not affect RNA structure, the pyridyl modification may contribute to Cu^{2+} coordination that slightly enhances DA_TR96 catalysis of MCA–AHEG through a mechanism analogous to that observed for DNA intercalated by Cu^{2+} chelators (50,51).

We propose that the DA_TR96 RNA acts as a scaffold, providing the structural constraints to allow rate acceleration of the MCA-AHEG Diels–Alder reaction by the hydrophobic effect with modest enhancement from Cu^{2+}. Accordingly, the sequence of the DA22 family of RNAs might be less important than the actual structures they form in solution and the number and positioning of pyridine modifications on the RNA surface. The original selection of the DA22 family of modified RNAs sought a metal ion chelation mechanism in the experimental design (21,39,40). However, the lack of a structural role for Cu^{2+} and modest kinetic effect of Cu^{2+} in our experiments agrees with previous work suggesting that ligation of Cu^{2+} in aqueous solution results in only modest rate enhancements in the most favorable geometries (49–51). On the other hand, the hydrophobicity of the pyridyl modification in DA_TR96 is sufficient to provide a surface for Diels–Alder catalysis since this reaction is known to be driven by hydrophobic interactions in water. These considerations suggest that a broad class of Diels–Alder substrates might be amenable to catalysis by the DA22 family of RNAs in a manner largely dependent on hydrophobicity. However, this possibility must be balanced with the lower solubility of the ribozyme in water. The structural complications of hydrophobic groups in aqueous solvent may explain why, with the extremely rare exception of the isopentenyl-aminomethyl moiety, a methyl group is the largest hydrophobic group found in naturally modified nucleosides (52).

Although progress has been made, there are still few examples to support the correlation of added chemical functionality with greater specificity and activity in nucleic acid aptamers and catalysts, respectively. The example from Battersby *et al.* (16), selecting an ATP aptamer, showed that the selection ignored the opportunity to use a cationic ammonium functionality. Ting *et al.* (23) have suggested that the step-up in functional potential will come when at least two different functionalities are incorporated into a single modified RNA or DNA. While certain modifications to RNA or DNA are hypothesized to mimic the functions of amino acid side chains in proteins, introduction of hydrophobic modifications would be expected to lead to hydrophobic pockets on the RNA surface or within folded RNA structure. The pyridyl side chain is an interesting combination of a hydrophobic group with the weak basicity of a nitrogen lone pair in an aromatic ring.

There are two major possible functional outcomes of an RNA modified with the pyridyl group that can be placed in context by analogy with metalloenzymes. The pyridyl groups could chelate a metal ion that would play a

structural and functional role in catalysis like that in metalloenzymes such as cytochrome c oxidase, where highly specific chelation of Cu^{1+}/Cu^{2+} is key to the mechanism. Alternatively, spatial organization of the hydrophobic modification on the RNA surface could lead to sequestration of hydrophobic substrates. By analogy, the hydrophobic binding pockets of the cytochrome P450 superfamily can accommodate a wide range of hydrophobic substrates (53,54). The flexibility of binding is essential to P450 function in the liver of mammals, for example, since a few hundred different enzymes must be capable of oxidizing tens of thousands of different substrates that enter the body to efficiently remove these molecules from the blood stream. However, this flexibility also permits adventitious binding and oxidation of polyaromatic hydrocarbons by certain cytochrome P450s leading to carcinogenesis (55,56). Thus, binding driven principally by the hydrophobic effect is a double-edged sword that can promote enzymatic catalysis for a class of substrates, but can simultaneously result in unintended outcomes.

In summary, the plasticity of a hydrophobic binding site can be a valuable design feature for the catalysis of a wide range of Diels–Alder substrates that may help overcome the problem of product inhibition. However, in order to achieve efficient catalysis, the design of the selection should also take into account the compatibility of the hydrophobic group with the structural stability of the RNA molecule and the possible unintended interactions with substrates. It is hoped that these structural observations will aid in the design of RNAs with modified side chains.

SUPPLEMENTARY DATA

Supplementary Data is available at NAR Online.

ACKNOWLEDGEMENTS

We thank Dr. Bruce Novak for PVHP and Dr. Bruce E. Eaton for advice and material that initiated the MS Thesis work of Ms. Showyi Ju. We also thank Mr. Richard Guenther for advice and training.

FUNDING

W.M. Keck Foundation (to S.F.); National Science Foundation (MCB 0543741 to E.S.M.). Funding for open access charge: W.M. Keck Foundation.

Conflict of interest statement. None declared.

REFERENCES

1. Kruger,K., Grabowski,P.J., Zaug,A.J., Sands,J., Gottschling,D.E. and Cech,T.R. (1982) Self-splicing RNA: Autoexcision and autocyclization of the ribosomal RNA intervening sequence of tetrahymena. *Cell*, **31**, 147–157.
2. Guerrier-Takada,C., Gardiner,K., Marsh,T., Pace,N. and Altman,S. (1983) The RNA moiety of ribonuclease P is the catalytic subunit of the enzyme. *Cell*, **35**, 849–857.
3. Ellington,A.D. and Szostak,J.W. (1990) In vitro selection of RNA molecules that bind specific ligands. *Nature*, **346**, 818–822.
4. Tuerk,C. and Gold,L. (1990) Systematic evolution of ligands by exponential enrichment – RNA ligands to bacteriophage-T4 DNA-polymerase. *Science*, **249**, 505–510.
5. Stoltenburg,R., Reinemann,C. and Strehlitz,B. (2007) SELEX-A (r)evolutionary method to generate high-affinity nucleic acid ligands. *Biomol. Eng.*, **24**, 381–403.
6. Seelig,B. and Jaschke,A. (1999) A small catalytic RNA motif with Diels-Alderase activity. *Chem. Biol.*, **6**, 167–176.
7. Chandra,M. and Silverman,S.K. (2008) DNA and RNA can be equally efficient catalysts for carbon-carbon bond formation. *J. Am. Chem. Soc.*, **130**, 2936–2937.
8. Stahley,M.R. and Strobel,S.A. (2006) RNA splicing: group I intron crystal structures reveal the basis of splice site selection and metal ion catalysis. *Curr. Opin. Struct. Biol.*, **16**, 319–326.
9. Lehmann,K. and Schmidt,U. (2003) Group II introns: structure and catalytic versatility of large natural ribozymes. *Crit. Rev. Biochem. Mol. Biol.*, **38**, 249–303.
10. Ban,N., Nissen,P., Hansen,J., Moore,P.B. and Steitz,T.A. (2000) The complete atomic structure of the large ribosomal subunit at 2.4 angstrom resolution. *Science*, **289**, 905–920.
11. Scott,W.G., Finch,J.T. and Klug,A. (1995) The crystal-structure of an all-RNA hammerhead ribozyme - a proposed mechanism for RNA catalytic cleavage. *Cell*, **81**, 991–1002.
12. Marquez,S.M., Chen,J.L., Evans,D. and Pace,N.R. (2006) Structure and function of eukaryotic ribonuclease P RNA. *Mol. Cell*, **24**, 445–456.
13. Valadkhan,S. and Manley,J.L. (2001) Splicing-related catalysis by protein-free snRNAs. *Nature*, **413**, 701–707.
14. Breaker,R.R. (1997) DNA enzymes. *Nat. Biotechnol.*, **15**, 427–431.
15. Narlikar,G.J. and Herschlag,D. (1997) Mechanistic aspects of enzymatic catalysis: lessons from comparison of RNA and protein enzymes. *Ann. Rev. Biochem.*, **66**, 19–59.
16. Battersby,T.R., Ang,D.N., Burgstaller,P., Jurczyk,S.C., Bowser,M.T., Buchanan,D.D., Kennedy,R.T. and Benner,S.A. (1999) Quantitative analysis of receptors for adenosine nucleotides obtained via in vitro selection from a library incorporating a cationic nucleotide analog. *J. Am. Chem. Soc.*, **121**, 9781–9789.
17. Keefe,A.D. and Cload,S.T. (2008) SELEX with modified nucleotides. *Curr. Opin. Chem. Biol.*, **12**, 448–456.
18. Latham,J.A., Johnson,R. and Toole,J.J. (1994) The application of a modified nucleotide in aptamer selection - novel thrombin aptamers containing 5-(1-pentynyl)-2′-deoxyuridine. *Nucleic Acids Res.*, **22**, 2817–2822.
19. Perrin,D.M., Garestier,T. and Helene,C. (2001) Bridging the gap between proteins and nucleic acids: a metal-independent RNAseA mimic with two protein-like functionalities. *J. Am. Chem. Soc.*, **123**, 1556–1563.
20. Santoro,S.W., Joyce,G.F., Sakthivel,K., Gramatikova,S. and Barbas,C.F. (2000) RNA cleavage by a DNA enzyme with extended chemical functionality. *J. Am. Chem. Soc.*, **122**, 2433–2439.
21. Tarasow,T.M., Tarasow,S.L. and Eaton,B.E. (1997) RNA-catalysed carbon-carbon bond formation. *Nature*, **389**, 54–57.
22. Vaish,N.K., Larralde,R., Fraley,A.W., Szostak,J.W. and McLaughlin,L.W. (2003) A novel, modification-dependent ATP-binding aptamer selected from an RNA library incorporating a cationic functionality. *Biochemistry*, **42**, 8842–8851.
23. Ting,R., Thomas,J.M., Lermer,L. and Perrin,D.M. (2004) Substrate specificity and kinetic framework of a DNAzyme with an expanded chemical repertoire: a putative RNaseA mimic that catalyzes RNA hydrolysis independent of a divalent metal cation. *Nucleic Acids Res.*, **32**, 6660–6672.
24. Hollenstein,M., Hipolito,C.J., Lam,C.H. and Perrin,D.M. A self-cleaving DNA enzyme modified with amines, guanidines and imidazoles operates independently of divalent metal cations (M^{2+}). *Nucleic Acids Res.*, Advance Access published on January 19, 2009; doi: 10.1093/nar/gkn1070.
25. Nicolaou,K.C., Snyder,S.A., Montagnon,T. and Vassilikogiannakis,G. (2002) The Diels-Alder reaction in total synthesis. *Angew. Chem. Intl. Ed.*, **41**, 1668–1698.
26. Corey,E.J. and Cheng,X.-M. (1989) *The Logic of Chemical Synthesis*, Wiley, New York, NY.

27. Morris,K.N., Tarasow,T.M., Julin,C.M., Simons,S.L., Hilvert,D. and Gold,L. (1994) Enrichment for RNA molecules that bind a Diels-Alder transition-state analog. *Proc. Natl Acad. Sci. USA*, **91**, 13028–13032.
28. Tarasow,T.M., Kellogg,E., Holley,B.L., Nieuwlandt,D., Tarasow,S.L. and Eaton,B.E. (2004) The effect of mutation on RNA Diels-Alderases. *J. Am. Chem. Soc.*, **126**, 11843–11851.
29. Seelig,B., Keiper,S., Stuhlmann,F. and Jaschke,A. (2000) Enantioselective ribozyme catalysis of a bimolecular cycloaddition reaction. *Angew. Chem.-Intl. Ed.*, **39**, 4576–4579.
30. Keiper,S., Bebenroth,D., Seelig,B., Westhof,E. and Jaschke,A. (2004) Architecture of a Diels-Alderase ribozyme with a preformed catalytic pocket. *Chem. Biol.*, **11**, 1217–1227.
31. Serganov,A., Keiper,S., Malinina,L., Tereshko,V., Skripkin,E., Hobartner,C., Polonskaia,A., Phan,A.T., Wombacher,R., Micura,R. *et al.* (2005) Structural basis for Diels-Alder ribozyme-catalyzed carbon-carbon bond formation. *Nat. Struct. Mol. Biol.*, **12**, 218–224.
32. Chiorcea-Paquim,A.M., Piedade,J.A.P., Wombacher,R., Jaschke,A. and Oliveira-Brett,A.M. (2006) Atomic force microscopy and anodic voltammetry characterization of a 49-mer Diels-Alderase ribozyme. *Anal. Chem.*, **78**, 8256–8264.
33. Kobitski,A.Y., Nierth,A., Helm,M., Jaschke,A. and Nienhaus,G.U. (2007) Mg^{2+}-dependent folding of a Diels-Alderase ribozyme probed by single-molecule FRET analysis. *Nucleic Acids Res.*, **35**, 2047–2059.
34. Wombacher,R., and Jaschke,A. (2008) Probing the active site of a Diels-Alderase ribozyme by photoaffinity cross-linking. *J. Am. Chem. Soc.*, **130**, 8594–8595.
35. Heine,A., Stura,E.A., Yli-Kauhaluoma,J.T., Gao,C.S., Deng,Q.L., Beno,B.R., Houk,K.N., Janda,K.D. and Wilson,I.A. (1998) An antibody exo Diels-Alderase inhibitor complex at 1.95 angstrom resolution. *Science*, **279**, 1934–1940.
36. Romesberg,F.E., Spiller,B., Schultz,P.G. and Stevens,R.C. (1998) Immunological origins of binding and catalysis in a Diels-Alderase antibody. *Science*, **279**, 1929–1933.
37. Hugot,M., Bensel,N., Vogel,M., Reymond,M.T., Stadler,B., Reymond,J.L. and Baumann,U. (2002) A structural basis for the activity of retro-Diels-Alder catalytic antibodies: Evidence for a catalytic aromatic residue. *Proc. Natl Acad. Sci. USA*, **99**, 9674–9678.
38. Breslow,R. (1991) How do imidazole groups catalyze the cleavage of RNA in enzyme models and in enzymes - evidence from negative catalysis. *Acc. Chem. Res.*, **24**, 317–324.
39. Tarasow,T.M., Tarasow,S.L. and Eaton,B.E. (2000) RNA Diels-Alderases: relationships between unique sequences and catalytic function. *J. Am. Chem. Soc.*, **122**, 1015–1021.
40. Tarasow,T.M., Tarasow,S.L., Tu,C., Kellogg,E. and Eaton,B.E. (1999) Characteristics of an RNA Diels-Alderase active site. *J. Am. Chem. Soc.*, **121**, 3614–3617.
41. Gagnon,K.T., Zhang,X.X., Agris,P.F. and Maxwell,E.S. (2006) Assembly of the archaeal box C/D sRNP can occur via alternative pathways and requires temperature-facilitated sRNA remodeling. *J. Mol. Biol.*, **362**, 1025–1042.
42. Bhattacharya,S. and Mandal,S.S. (1997) Interaction of surfactants with DNA. Role of hydrophobicity and surface charge on intercalation and DNA melting. *Biochim. Biophys. Acta. Biomem.*, **1323**, 29–44.
43. Tan,W.B., Bhambhani,A., Duff,M.R., Rodger,A. and Kumar,C.V. (2006) Spectroscopic identification of binding modes of anthracene probes and DNA sequence recognition. *Photochem. Photobiol.*, **82**, 20–30.
44. Zuker,M. (2003) Mfold web server for nucleic acid folding and hybridization prediction. *Nucleic Acids Res.*, **31**, 3406–3415.
45. Tran,E.J., Zhang,X.X. and Maxwell,E.S. (2003) Efficient RNA 2′-O-methylation requires juxtaposed and symmetrically assembled archaeal box C/D and C′/D′ RNPs. *EMBO J.*, **22**, 3930–3940.
46. Hofacker,I.L., Fekete,M. and Stadler,P.F. (2002) Secondary structure prediction for aligned RNA sequences. *J. Mol. Biol.*, **319**, 1059–1066.
47. Batey,R.T., Gilbert,S.D. and Montange,R.K. (2004) Structure of a natural guanine-responsive riboswitch complexed with the metabolite hypoxanthine. *Nature*, **432**, 411–415.
48. Rideout,D.C. and Breslow,R. (1980) Hydrophobic acceleration of Diels-Alder reactions. *J. Am. Chem. Soc.*, **102**, 7816–7817.
49. Otto,S. and Engberts,J. (1999) A systematic study of ligand effects on a Lewis-acid-catalyzed Diels-Alder reaction in water. Water-enhanced enantioselectivity. *J. Am. Chem. Soc.*, **121**, 6798–6806.
50. Boersma,A.J., Klijn,J.E., Feringa,B.L. and Roelfes,G. (2008) DNA-based asymmetric catalysis: sequence-dependent rate acceleration and enantioselectivity. *J. Am. Chem. Soc.*, **130**, 11783–11790.
51. Roelfes,G., Boersma,A.J. and Feringa,B.L. (2006) Highly enantioselective DNA-based catalysis. *Chem. Commun.*, 635–637
52. Limbach,P.A., Crain,P.F. and McCloskey,J.A. (1994) Summary: the modified nucleosides of RNA. *Nucleic Acids Res.*, **22**, 2183–2196.
53. Xu,L.H., Fushinobu,S., Ikeda,H., Wakagi,T. and Shoun,H. (2009) Crystal structures of cytochrome P450 105P1 from *Streptomyces avermitilis*: conformational flexibility and histidine ligation state. *J. Bacteriol.*, **191**, 1211–1219.
54. Ekins,S. (2004) Predicting undesirable drug interactions with promiscuous proteins in silico. *Drug Discov. Today*, **9**, 276–285.
55. Adams,J.D., Yagi,H., Levin,W. and Jerina,D.M. (1995) Stereoselectivity and regioselectivity in the metabolism of 7,8-dihydrobenzo[a]pyrene by cytochrome-P450, epoxide hydrolase and hepatic microsomes from 3-methylcholanthrene-treated rats. *Chem. Biol. Interact.*, **95**, 57–77.
56. Boyd,G.W., Young,R.J., Harvey,R.G., Coombs,M.M. and Ioannides,C. (1993) The metabolism and activation of 15,16-dihydrocyclopenta[a]phenanthren-17-one by cytochrome-P-450 proteins. *Eur. J. Pharmacol. Env. Tox. Pharm. Sect.*, **228**, 275–282.